Chemistry – A European Journal

Research Article

Structural Dissection of Epsin-1 N-Terminal Helical Peptide: The Role of Hydrophobic Residues in Modulating Membrane Curvature

Motoki Nishimura,[a] Yoshimasa Kawaguchi,[a] Kakeru Kuroki,[a] Yuna Nakagawa,[a] Toshihiro Masuda,[a] Takayuki Sakai,[a] Kenichi Kawano,[a] Hisaaki Hirose,[a] Miki Imanishi,[a] Tomoka Takatani-Nakase, [b,c] Sergii Afonin,[d] Anne S. Ulrich,[d,e] Shiroh Futaki*[a]

[a] M. Nishimura, Dr. Y. Kawaguchi, K. Kuroki, Nakagawa, Dr. T. Masuda, Dr. T. Sakai, Dr. K. Kawano, Dr. H. Hirose, Dr. M. Imanishi, Prof. Dr. S. Futaki

Institute for Chemical Research, Kyoto University

Uji, Kyoto 611-0011, Japan.

futaki@scl.kyoto-u.ac.jp

https://www.scl.kyoto-u.ac.jp/~bfdc/index.html

Twitter: @futaki_lab; @kuicr_kaken; @Hi_Hisaaki

[b] Prof. Dr. T. Takatani-Nakase

School of Pharmacy and Pharmaceutical Sciences, Mukogawa Women's University

Nishinomiya, Hyogo 663-8179, Japan

[c] Prof. Dr. T. Takatani-Nakase

Institute for Bioscience, Mukogawa Women's University

Nishinomiya, Hyogo 663-8179, Japan

[d] Dr. S. Afonin, Prof. Dr. A. S. Ulrich

Institute of Biological Interfaces (IBG-2), Karlsruhe Institute of Technology (KIT)

P.O.B. 3640, 76021 Karlsruhe, Germany.

[e] Prof. Dr. A. S. Ulrich

Institute of Organic Chemistry (IOC), Karlsruhe Institute of Technology (KIT),

Fritz-Haber-Weg 6, 76131 Karlsruhe, Germany.

Supporting information for this article is given via a link at the end of the document.

Abstract

Spatiotemporal structural alterations in cellular membranes are the hallmark of many vital processes. In these cellular events, the induction of local changes in membrane curvature often plays a pivotal role. Many amphiphilic peptides are able to modulate membrane curvature, but there is little information on specific structural factors that direct the curvature change. Epsin-1 is a representative protein thought to initiate invagination of the plasma membrane upon clathrin-coated vesicles formation. Its N-terminal helical segment (EpN18) plays a key role in inducing positive membrane curvature. This study aimed to elucidate the essential structural features of EpN18 in order to better understand general curvature-inducing mechanisms, and to design effective tools for rationally controlling membrane curvature. Structural dissection of peptides derived from EpN18 revealed the decisive contribution of hydrophobic residues to (i) enhancing membrane interactions, (ii) helix structuring, (iii) inducing positive membrane curvature, and (iv) loosening lipid packing. The strongest effect was attained by substitution with leucine residues, as this EpN18 analog showed a marked ability to promote the influx of octa-arginine cell-penetrating peptides into living cells.

Introduction

Dynamic deformation of cellular membranes such as membrane fusion, fission, division, endoplasmic reticulum and Golgi formation, underline various cellular phenomena such as cell motility, cell division and membrane trafficking.[1] These cellular processes are crucial for cellular life. Although structures of lipids composing biological membranes directly affect membrane structures to yield curvatures, it is known that membrane-interacting peptides and proteins also play a significant role in modulating membrane structure.[2] Insertion of certain amphiphilic helix peptide segments induces positive membrane curvature, as seen in the membrane interactions of epsin and sar1p.[3] Scaffolding proteins, including BAR (Bin/Amphiphysin/Rvs) domain proteins, are also known to generate generate curvature actively.[4] Curvature-modulating peptides that cause elevated membrane permeabilization are potentially applicable to facilitate drug delivery[5] or to promote endocytosis.[6] Cytotoxic (e.g. antimicrobial, antifungal, and antiviral peptides) having membrane lysis activity often demonstrate, in association, a solid positive curvature-inducing action.[7] Additionally, not only membrane-sculpturing proteins but also proteins that more passively sense membrane curvatures (e.g., those having amphiphilic lipid packing sensor (ALPS) motifs) play a functional role in modulating membrane vesicle trafficking in cells.[8] Developing a method or a tool to modulate cell membrane curvature in a rational manner should thus open up various ways to control cellular phenomena artificially.

Epsin-1 is a highly conserved cellular protein involved in the formation of clathrin-coated pits during endocytosis.[3b, 9] We have previously shown that EpN18, an 18-residue peptide derived from the N-terminal amphipathic region of epsin-1 (Figure 1A and S1), induces positive membrane curvature and causes membrane budding in giant unilamellar vesicles.[10] When applied from the outside of a cell, EpN18 also induces a loosening of the lipid packing in the outer leaflet of the plasma membrane, which facilitates translocation of octa-arginine cell-penetrating peptides (R8) across the membrane into the cytosol.[5c]

The ability of EpN18 to induce positive curvature is attributed to the shallow insertion of its amphiphilic helix into the lipid bilayer.[1, 8, 11] When the hydrophobic face binds this way, steric crowding amongst the surrounding lipids may lead to an increase in the surface area of the peptide-exposed leaflet of the bilayer, yielding a positive curvature and loosening the overall lipid-packing (Figure 1B).[11a] By elucidating the underlying structural basis of how EpN18 is able to modulate membrane curvature, new peptide-based tools can be generated for intentionally controlling numerous cellular phenomena without any change in lipid composition. Along this line, we have recently shown that multimerization and membrane anchoring of EpN18 leads to an enhanced interaction with membranes.[12],[13] However, the structural features that specifically contribute to curvature induction and membrane sculpturing by EpN18 remain elusive. It has been reported that various cellular proteins involved in regulating membrane curvature likely share a common curvature-inducing mechanism, namely through

the interaction of N-terminal amphiphilic helices with the membranes.[14],[15] Molecular dynamics (MD) simulations are tools well-suited to estimate the fine details of the molecular interplay of peptides with membranes at atomic resolution.[16] Lipid packing defects in the membrane are characterized by the exposure of the lipid molecules' hydrophobic parts to the membrane's surface. The hydrophobic interactions of peptides with the lipid packing defects attain curvature sensing, such as by ALPS sequences. Although marked structural alterations of lipid bilayers do not accompany these, as in the case of an active curvature induction; overall, the peptide folding at membrane interfaces is a slow process at the scale of molecular dynamics and has been so far poorly characterized.[17] More dramatic and, therefore, even slower changes of both peptides' and lipid bilayer structures occur when the curvature is actively induced; cooperative interactions of multiple peptide molecules with membranes are often involved. Hence, compared to the simulation studies on the peptide-based curvature sensing,[16b, 16h, 16i] much longer time scales or higher computation abilities are needed to depict the processes that underline peptide-mediated curvature induction correctly. Analysis by all-atom MD remains not easy even using current state-of-art computation systems. Models may be presented by coarse-grained simulations,[16e, 16f] however, questions remain about the relevance to real molecules.[7b, 17] Therefore, a better knowledge of the curvature-inducing mechanism by EpN18 using systematically designed analogs will impact

our understanding of membrane structure regulation mechanisms utilized by these proteins and peptides in general.

In the present study, we aimed to (i) understand the relationship between structural factors of EpN18 – in particular, the helix forming propensity and specific amino acid composition – and the ability to induce positive curvature; and to (ii) obtain fundamental knowledge allowing the rational design of positive curvature-inducing peptides.

Results and Discussion

Design of simplified peptides

Important structural aspects of amphiphilic helical peptides include hydrophobicity, helicity (α-helix content), charge, and balance of amphiphilicity (i.e. relative hydrophobic surface area). We thus designed compositionally simplified analogs of EpN18, with the intention to vary these features and to correlate the observed effects on curvature induction by means of physicochemical and cell biological evaluations.

Original EpN18 has a predicted α-helical structure (Figure 1A: XSTSSLRRQXKNIVHNYS-amide, where X = norleucine/Nle substitutes native methionine to avoid ambiguity in polarity upon sulfur oxidation).[10] EpN18 contains six hydrophobic amino acids, Nle^{1}, Leu^{6}, Nle^{10}, Ile^{13}, Val^{14}, and Tyr^{17} (Figure 1A). As seen in the helical wheel projection, the latter five residues constitute the hydrophobic face of an amphipathic helix. A relatively small hydrophobic face in EpN18, as in many other curvature-inducing helices, is believed to determine their rather shallow insertion into target membranes. This gentle way of binding contrasts the usually much deeper insertion seen by typical membranolytic peptides which tend to possess larger hydrophobic faces. The shallower insertion is less prone to cause bilayer rupture. Yet, it may still increase the surface area in the outer membrane leaflet and thereby generate positive membrane curvature (Figure 1B). The natural hydrophobic amino acid tryptophan is often employed as a probe to analyze membrane interactions of amphiphilic

peptides.[18] EpN18-L6W was thus designed as a benchmark peptide in this study, by replacing Leu^6 (which is located on the hydrophobic face of folded EpN18, see Figure 1A and Figure 2, top) with a tryptophan, allowing to quantify the interaction of the peptide with lipid bilayers through the changes in tryptophan fluorescence (Table 1).

EpN18 contains three basic amino acids (Arg^7, Arg^8, and Lys^{11}) and eight uncharged, polar residues (Ser^2, Thr^3, Ser^4, Ser^5, Gln^9, Asn^{12}, His^{15}, and Asn^{16}). As these amino acids are often not conserved in other curvature inducing/sensing amphiphilic helical peptides,[8, 16d, 19] the general properties of these side chains rather than the specific amino acid composition seems to be of prime importance.[20]

The helix-forming propensity can be a significant factor for curvature induction. Therefore, we studied the effect of specific amino acids on the helicity of EpN18. The conformational preferences of natural amino acid residues are well known from analyses of their occurrence in secondary structures of proteins.[21] Amongst the hydrophobic amino acids, leucine is frequently found in α-helical segments and thus considered to promote helicity.[22] On the same grounds, hydrophobic valine tends to occur in extended β-type conformations in peptides. Two analogs of EpN18-L6W were thus designed: EpN18-L and EpN18-V, in which all hydrophobic amino acids other than tryptophan were replaced with leucine or valine, respectively (Table 1, Figure 2). Amongst the polar amino acids, glutamine more often resides in α-helical structures, while threonine and serine prefer β-

strand and β-turn conformations, whereas asparagine is considered to be a "helix breaker".[21b] Therefore, EpN18-Q and EpN18-N were prepared as model peptides to examine the effect of a global replacement of polar non-charged residues with potentially increased and decreased helix-promoting propensities. In these peptides, all of the non-charged hydrophilic amino acids (Gln, Asn, Ser, Thr) were unified to either glutamine or asparagine. Considering basic amino acids, lysine is found slightly more frequently in helical sequences, whereas arginine is slightly less present.[21b] Overall, these cationic residues do not seem to prefer one or the other conformation pronouncedly. We nevertheless prepared EpN18-K and EpN18-R to complete the series of our peptides. In all EpN18 analogs, His^{15} was left unchanged, since it is located on the hydrophilic face, and because its unique pH-dependent character is not shared with any other amino acid. Note that the imidazole nitrogen of histidine ($pK^a \approx 6.0$)[23] is likely to be uncharged at neutral pH. All peptides were prepared by Fmoc solid-phase peptide synthesis[24] and purified by high-performance liquid chromatography.

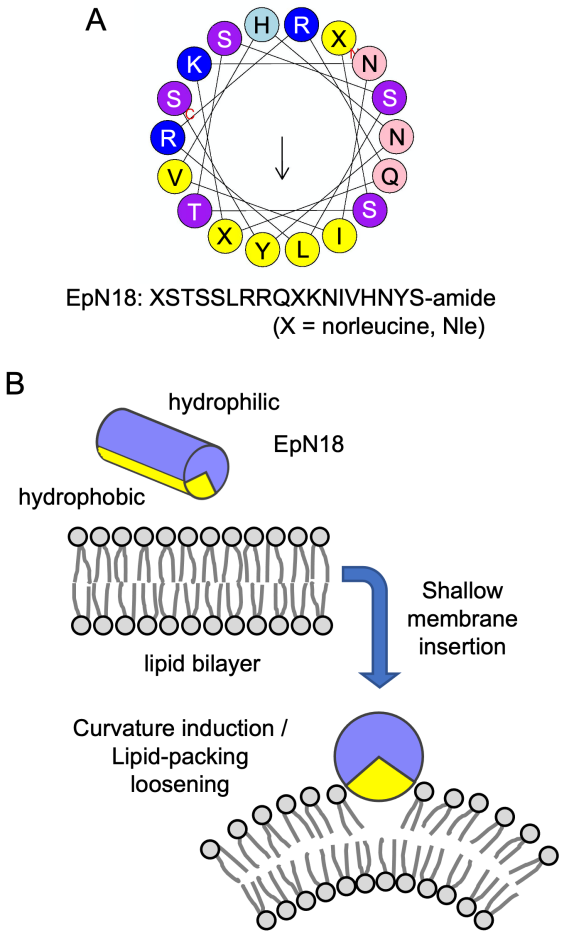

Fig. 1 (A) Helical wheel projection of EpN18. (B) Interaction of amphiphilic helical peptides to induce positive curvature and loosen lipid-packing.

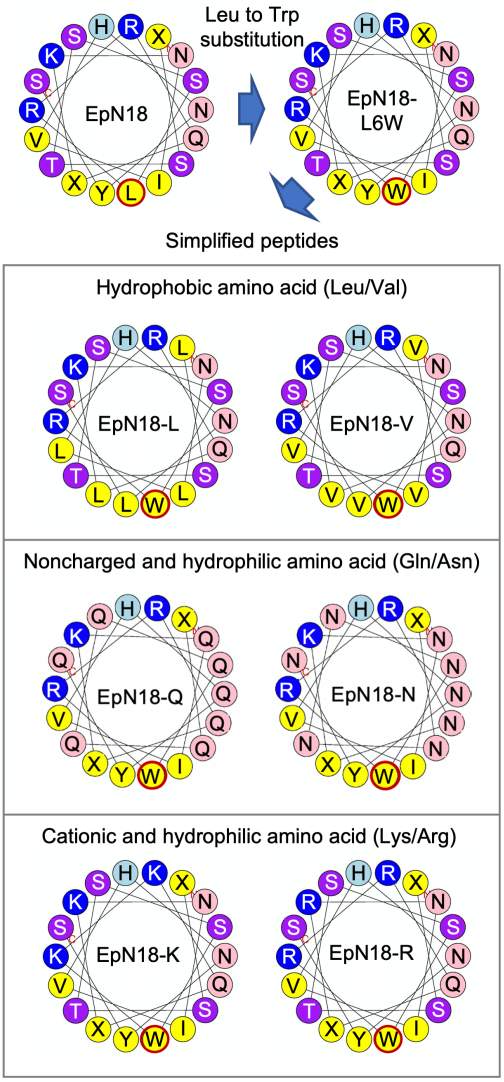

Fig. 2 Design of EpN18 analogs. Position 6 is highlighted with a red circle. Color codes for amino acids: yellow – hydrophobic [X = norleucine (Nle), L = leucine (Leu), I = isoleucine (Ile), V = valine (Val), and Y = tyrosine(Tyr)]; blue – basic [K = lysine (Lys), R = arginine (Arg)]; purple [S = serine (Ser), T = threonine (Thr)]; pink [N = asparagine (Asn), Q = glutamine (Gln)]; light blue [H = histidine (His)]. The images were drawn using the HeliQuest webserver (https://heliquest.ipmc.cnrs.fr/).[25]

Helix formation propensities of the peptides

The helix formation propensity of the synthesized peptides was assessed by circular dichroism (CD). In the CD spectrum, α-helical peptides have characteristic negative maxima at around 208 nm and 222 nm, and the molar ellipticity at 222 nm ($[\theta]_{222}$) can be used to estimate the helix content.[26] Tris buffer containing 20% trifluoroethanol (TFE) was employed as a solvent to compare the intrinsic helix propensity of each peptide sequence under conditions that are favorable to adopting a helix structure.[27] The CD spectra of all peptides other than EpN18-Q and EpN18-V suggest a significant helicity (Figure 3A). According to the $[\theta]_{222}$ values, EpN18-L6W retained a considerable helix-forming propensity despite its substitution of leucine with tryptophan, as only a moderate decrease in helicity was observed ($[\theta]_{222}$ for EpN18-L6W vs EpN18: -1.7×10^4 versus -2.6×10^4 deg cm^2 dmol^{-1}, respectively).

Peptides with substitutions of hydrophobic amino acids yielded helix propensities in the order of EpN18-L ($[\theta]_{222}$: -3.0×10^4 deg cm^2 dmol^{-1}) > EpN18-L6W (-1.7×10^4 deg cm^2 dmol^{-1}) > EpN18-V (-1.1×10^4 deg cm^2 dmol^{-1}), suggesting that the substitution of all hydrophobic amino acids with leucine indeed promotes the helicity (Table 1, $[\theta]_{222}$). EpN18-V not only had the lowest $[\theta]_{222}$ readout, but its short wavelength minimum was shifted to 206-207 nm due to a higher contribution of random non-helical conformations. Regarding the polar substitutions to glutamine and asparagine, EpN18-N showed an α-helical conformation, but its helix-propensity was much lower than that of EpN18-L6W.

The low absolute intensity ($[\theta]_{222}$: -6.7 × 10^3 deg cm^2 $dmol^{-1}$) along with a high scattering noise strongly suggest that this peptide aggregates even in 20% TFE solution. EpN18-Q showed no helix-like double minima, but instead a β-type spectrum, as suggested by the single minimum at 217 nm. We note that these fundamental conformational changes should be taken as a warning not to interfere too much with the underlying amphiphilic framework of the parent peptide, especially with a view to the uncharged polar substitutions. Therefore, we suggest that the hydrophilic residues in EpN18 should better be retained at their original positions, in order not to interfere with the peptide helicity. As for the charged amino acids, EpN18-R ($[\theta]_{222}$: -2.0× 10^4 deg cm^2 $dmol^{-1}$) exhibited a slightly higher helix content compared with EpN18-K ($[\theta]_{222}$: -1.7 × 10^4 deg cm^2 $dmol^{-1}$). However, these values are similar to that of EpN18-L6W. Therefore, we conclude that a substitution of basic amino acids may not yield much difference in helix propensity. Overall, the helix-forming propensities of the peptides were estimated in the order of EpN18-L > EpN18 > EpN18-R ≥ EpN18-L6W ≈ EpN18-K >> EpN18-V> EpN18-N>>>EpN18-Q. Only EpN18-L had a higher helix-forming propensity than EpN18 (See Figure S2 in Supporting Information illustrating ideal (most common rotamers) orientations of amino acid residues in EpN18 and EpN18-L under the assumption that the peptides are folded as 100% ideal α-helices).

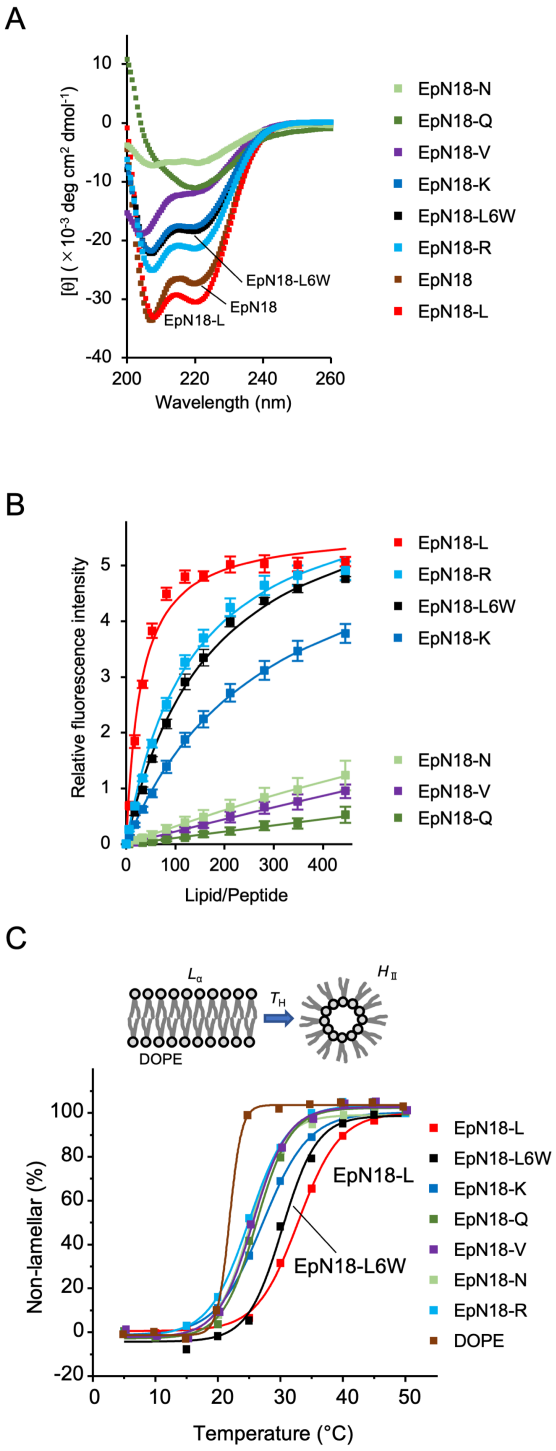

Fig. 3 (A) CD spectra, (B) binding curves to DOPC/DOPS (1:1) LUVs, and (C) scheme of L_a-to-H_{II} phase transition (upper insert) with temperature-dependent curves that show % non-lamellar lipid phase of DOPE as observed by ^{31}P-ssNMR in

presence of EpN18 analogs. The data of (B) are expressed as the mean value± SD of three experiments.

Membrane affinity, and hydrophobicity of the peptides

The ability of the peptides to interact with membranes was evaluated by an increase in fluorescence intensity of tryptophan at 325 nm, using large unilamellar vesicles (LUVs) comprised of 1-palmitoyl-2-oleoyl-*sn*-glycero-3-phosphocholine (POPC) and 1-palmitoyl-2-oleoyl-*sn*-glycero-3-phospho-L-serine (POPS) (1:1). The peptide concentration yielding 50% towards saturation was defined as $[L]_{1/2}$ and taken as a measure of membrane binding.[18] The resulting $[L]_{1/2}$ obtained by the Trp-binding assay are shown in Figure 3B and Table 1. EpN18-L had the lowest $[L]_{1/2,}$ followed by EpN18-R ≈ EpN18-L6W, and EpN18-K. EpN18-N, EpN18-V and EpN18-Q did not bind significantly to the negatively charged LUVs, corroborating the above CD results showing correspondingly decreased helix propensities.

In addition, the relative hydrophobicities of the peptides were assessed by measuring their retention times in analytical reverse-phase high-performance liquid chromatography (RP-HPLC). The order of elution has been suggested to correlate well with the hydrophobicity of the folded peptides, as molecules with a higher hydrophobicity should have a higher affinity to the HPLC stationary phase [28]. Here, the retention time of EpN18-L was the largest, and we observed an order of EpN18-L > EpN18-R ≥ EpN18 ≥ EpN18-L6W > EpN18-K > EpN18-Q > EpN18-N > EpN18-V (Table 1, R_t). Despite some minor differences, the general

order of hydrophobicity corresponds well with the observed decrease in the peptides' helicity (Table 1, $[\theta]_{222}$).

Curvature induction by the peptides in artificial membranes

EpN18 has been reported to have a pronounced ability to induce positive membrane curvature.[10] This property is conveniently analyzed by using solid-state ^{31}P-NMR to monitor the lamellar-to-inverted-hexagonal L_α-to-H_{II} lipid phase transition temperature of 1,2-dioleoyl-*sn*-glycero-3-phosphoethanolamine (DOPE). When peptides are reconstituted in mechanically oriented planar membrane samples, it is easy to read out the ^{31}P chemical shift anisotropy, which changes dramatically once the lipid matrix turns into an H_{II} phase at elevated temperature. Any peptide that increases the L_α-to-H_{II} phase transition temperature (T_H) of pure DOPE will tend to stabilize the planar lamellar phase relative to the negatively curved inverted hexagonal phase. By monitoring the temperature-dependent ^{31}P chemical shift anisotropy of DOPE, the tendency of a peptide to induce positive curvature can thus be quantified from the upward shift in the phase transition temperature, ΔT_H.[29]

In our measurements, again, EpN18-L yielded the highest ΔT_H of 10.7°C, followed by EpN18 (9.3°C) and EpN18-L6W (8.1°C) (Figure 3C, Table 1). EpN18-R had shown a higher helix propensity and slightly stronger membrane binding than EpN18-K, but in the curvature assay we note that the order of ΔT_H was reversed with EpN18-K being more effective (EpN18-K: 5.0°C; EpN18-R; 2.5°C). Altogether,

EpN18-K, EpN18-R, EpN18-V, EpN18-Q and EpN18-N maintained the ability to induce positive curvature; however, their ΔT_H values fell within a range of 2.5-5.0°C, which is significantly smaller than the changes induced by the original EpN18, the benchmark peptide EpN18-L6W, and the high-performer EpN18-L. We should note that in this experiment, the peptides were added to the lipid bilayer during sample preparation by means of co-solubilization, hence they are already bound and well balanced between the two monolayers. As they must be folded at this point, at least once the sample has been hydrated and equilibrated, neither the helix-forming propensity nor any difference in binding strength should contribute much to the curvature-inducing effect that is assessed in this ^{31}P-NMR experiment. These considerations emphasize the intrinsic curvature-inducing ability of the EpN18-L analog, which has outperformed all other peptides (including the original EpN18) due to its hydrophobic face being uniformly decorated with bulky, helix-promoting leucine residues. In the future, it should be interesting to find out how EpN18-I would have behaved in these experiments. Ile is thought to have a comparable hydrophobicity to Leu but possesses less helix-forming propensity than Leu. The study using EpN18-I may give clearer information on the importance of hydrophobicity and helicity for curvature induction by the EpN18-L peptide.

Owing to the poor performance of all other sequences besides EpN18, Epn18-L6W and Epn18-L, we decided to include only the latter three peptides in the following cell experiments.

Ability of the peptides to loosen lipid packing of plasma membranes

We had previously reported that the treatment of cells with EpN18 led to a pronounced loosening of the lipid packing in the plasma membrane, thereby facilitating the translocation of arginine-rich cell-penetrating peptides into the cytosol.[10], [5c] Here, we thus examined whether EpN18-L had a similar effect, possibly with a higher activity compared to EpN18. As previously reported, HeLa cells were treated with EpN18, EpN18-L6W and EpN18-L (40 μM each), and the effects on lipid-packing of cell membrane were evaluated from ΔGP analysis using environment-responsive fluorescent probe di-4-ANEPPDHQ, where a decrease in GP values can demonstrate and quantify loosening of the lipid packing.[30]

EpN18 had been reported to decrease the GP value,[5c] and in the present experiment EpN18-L6W yielded a comparable ΔGP (Figure 4A). A more significant decrease was observed for EpN18-L treated cells, which was in accord with the above tendency that EpN18-L6W possess the highest curvature-inducing power (Figure 4A).

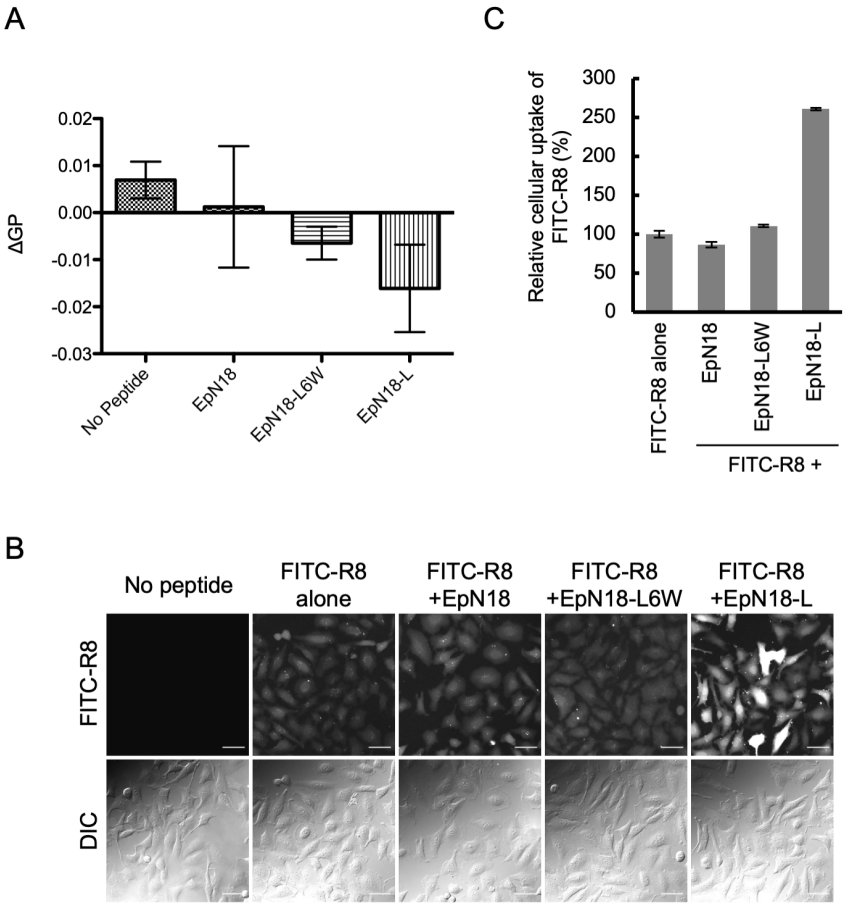

Fig. 4 (A) ΔGPs of cell membranes treated with EpN18 analogs (40 μM) for 5 min. The data are expressed as the mean value ± SE of three experiments. (B) CLSM observation, and (C) flow cytometry analysis of the cells treated with 10 μM FITC-R8 in the absence and presence of EpN18 analogs (40 μM each) for 5 min. Scale bar: 50 μm. The data are expressed as the mean value ± SE of three experiments.

Ability of the peptides to promote membrane translocation of octa-arginine

The generation of lipid packing defects by the interaction of EpN18 and other curvature-inducing peptides has been reported to promote direct translocation of octa-arginine (R8), a representative non-amphipathic cell-penetrating peptide, through plasma membrane into the cytosol without using endocytosis.[10],[5c] Following the same procedures as in these papers (see Supporting Information for details), we confirmed the cytosolic translocation of R8-labelled with fluorescein isothiocyanate (FITC-R8) in the presence of EpN18 with 5 min co-incubation (final concentrations, 10 and 40 μM, respectively), using confocal laser scanning microscopy (CLSM) (Figure S3).

Treatment with FITC-R8 alone yielded very few cells that would exhibit any cytosolic FITC-R8 signals (Figure S3). In the presence of EpN18 and EpN18-L6W, numerous cells showed marked diffuse cytosolic FITC-R8 signals, as reported for EpN18 previously (Figure S3).[10] Interestingly, the addition of EpN18-L led to significant cell death, thus yielding poor internalized FITC-R8 signals (Figure S3 and Figure S4A). Considering that a concentration of 40 μM of EpN18-L alone, which was employed for GP analysis in Figure 4, yielded no significant cytotoxicity (Figure S4A), cell death must have occurred due to synergistic membrane interactions of FITC-R8 and EpN18-L.

In the above cell experiments, EpN18 analogs were added from 4x concentrated stock solutions (50 μL were added to 150 μL culture medium covering the cells, i.e. 1:3 dilution) to yield the final peptide concentrations of FITC-R8 and EpN18-L (10 and 40μM, respectively). To compare EpN18 and EpN18-L in promoting

cytosolic translocation of FITC-R8 while avoiding the cytotoxicity noted above, we now removed the culture medium covering the cells and then added the medium containing FTIC-R8 and EpN18 of the final concentrations (Figure 4B). Using this protocol, cytotoxicity was considerably lower, yielding no significant cell death upon treatment with 10 μM FITC-R8 in the presence of 40 μM EpN18-L (Figure S3B).

Using the improved protocol, we did not observe any significant change of FITC-R8 uptake in the presence of EpN18 or EpN18-L6W (Figure 4B), compared to the old protocol. On the other hand, EpN18-L yielded a marked increase in cytosolic FITC-R8 signals (Figure 4B). A comparison of the relative cellular uptake of FITC-R8 in the presence of the respective EpN18 analogs using flow cytometry showed a similar trend (Figure 4C): a 2.5-fold uptake of FITC-R8 was attained in the presence of EpN18-L6W, compared to its absence or in the presence of EpN18 or EpN18-L6W. This finding was in accord with the higher lipid-packing loosening ability of EpN18-L compared to EpN18 and EpN18-L6W. Note that no significant changes in the cellular structures nor any obvious cellular damage were observed upon treatment with these peptides (Figure 4B), suggesting the cytosolic influx of FITC-R8 was not due to massive membrane rupture caused by these peptides. Here, the FITC moiety can be regarded as a model compound representing a small molecular weight cargo attached to R8. Therefore, it is conceivable that improved cytosolic delivery can be achieved using curvature-modulating peptides possessing a strong activity in terms of non-destructive loosening of the plasma

membrane lipid packing. At the same time, any cytotoxic effects obviously need to be closely examined.

Conclusions

In this study, we designed and synthesized EpN18 analogs to clarify the structural features contributing to the curvature-inducing activity of amphiphilic α-helical peptides. We investigated the relationship between hydrophobicity and helicity, and were able to correlate these properties of EpN18 analogs with their abilities to induce positive membrane curvature and perturb the packing of membrane lipids. The analog EpN18-L has the highest hydrophobicity and intrinsic helicity among all studied peptides, and it shows the strongest activity in terms of curvature induction and loosening of lipid-packing. Furthermore, this peptide promoted cytosolic translocation of R8 through the cell membrane, being significantly more effectively than the parent EpN18. As a conclusion from these studies, we also realized that a benign membrane-sculpturing peptide can be turned into a harmful membranolytic one once the membrane interactions become too strong. A particular aim for future investigations should thus lead to a further fine-tuning of structural modifications in curvature-inducing peptides, so that their optimum range can be delineated. It would be interesting to confirm how transferable the results obtained in this study are to other curvature-modulating peptides or membrane-active peptides in general. A better understanding of these peptide-membrane interactions will lead to more rational approaches to modulate membrane curvature using peptides. Such tools should help to accurately regulate cellular phenomena related to membrane re-organization and facilitate intracellular drug delivery.

Experimental Section

Preparation of oriented membrane samples

Oriented membrane samples for solid-state ^{31}P-NMR measurements were prepared by hydrating the 1:100 (mol:mol) peptide:DOPE (1,2-dioleoyl-*sn*-glycero-3-phosphoethanolamine) mixtures on glass supports, as described previously.[12, 31] Briefly, the peptides were dissolved in methanol at room temperature (~23 °C), the lipid in 9:1 chloroform:methanol at 48 °C. From the stock solutions, appropriate aliquots of peptide and lipid were combined in excess 1:1 chloroform:methanol solution (ca. 200 µL). The resulting mixtures were deposited onto six ultrathin (12 × 7.5 × 0.08 mm) glass slides (Paul Marienfeld). Total of 3.0 mg lipid was used for each sample. The slides were dried under vacuum overnight and rehydrated for 16-24 h in a sealed plastic container in the saturated water atmosphere (at 4 °C, below the T_H). The stacks were insulated by wrapping them with parafilm® and a polyethylene foil. Oriented samples were kept on ice before the NMR measurements.

Solid-state ^{31}P-NMR spectroscopy

Solid-state ^{31}P-NMR experiments were performed on a wide-bore AVANCEIII spectrometer (Bruker), operating for ^{31}P at 202.46 MHz. The spectra were recorded

using a Bruker static triple-resonance (HX(Y)) probe, employing a standard Hahn-echo pulse sequence and a two-pulse phase-modulated ^{1}H-decoupling (Bruker TPPM-20 decoupling sequence, 30 kHz). The X-channel 90° pulse length of 4 µs, echo-delay time of 30 µs, and a recycle time of 4 s were applied. Standard temperature regulating equipment of the spectrometer was used, automatically controlling the sample temperature by heating an externally cooled airflow (1600 L/h). The explored temperature ranged nominally between 278-323 K in 5 K temperature steps) For each spectrum, at least 256 scans were accumulated, using a 600 s pre-acquisition delay for the temperature equilibration. The processing was performed by using standard Bruker TopSpin software. Temperature-dependent curves characterizing the L_{α}-to-H_{II} phase transition of DOPE (Figure 3C) have been fitted with a logistic function (sigmoid curve) using OriginPro 2021b software.

Analysis of GP value by di-4-ANEPPDHQ imaging

Di-4-ANEPPDHQ (excited by 488-nm laser) is a membrane-staining dye that can be used to visualize membrane disorder utilizing its red shift in the fluorescence emission at 510-550 nm and 630-670 nm.[5c, 30] The shift level is recognized as generalized polarization (GP) value after being analyzed by a ratiometric measurement, as

$$\mathbf{GP} = \frac{\boldsymbol{I}_{\mathbf{510-550}} - \boldsymbol{I}_{\mathbf{630-670}}}{\boldsymbol{I}_{\mathbf{510-550}} + \boldsymbol{I}_{\mathbf{630-670}}}$$

A decrease in GP value suggests the increase of polarity or loosening of the lipid packing. The measurement was started from HeLa cells (2.0×10^5) plated onto 35-mm glass-bottomed dishes (Iwaki) and cultured in α-MEM(+) at 37 °C under 5 % CO_2 for 48 h. Cells were twice washed with α-MEM(–) prior to the incubation of 5 μM di-4-ANEPPDHQ in 150 μL serum-free α-MEM [α-MEM(−)] at 37 ° C under 5 % CO_2 for 10 min. Then, cells were settled in the incubator (humidified atmosphere at 37 °C) on Olympus FV1000 CLSM equipped with a standard 60× objective and incubated for 10 min for stabilization. Images were obtained every 1 min from −3 min before adding peptide solution in α-MEM(−) (50 μL) containing 1 % DMSO. After the microscopic observation, following the method reported by Owen *et al.*,[30] the images were subsequently processed using Image J 1.48v to acquire pseudo-colored GP images. To determine changes in the GP on the cell membranes, the peripheral area of a cell was selected as a region of interest (ROI), and the mean GP of the membrane region for each cell was obtained. After determining the GP value, the difference in GP (ΔGP) between before (average of –3, –2, and –1 min) and after (10 min) the peptide treatment was calculated.

Confocal microscopy of R8 internalization

HeLa cells (2.0×10^5) were plated onto 35-mm glass-bottomed dishes and cultured in α-MEM(+) at 37 °C under 5 % CO_2 for 24 h. Cells were twice washed with α-MEM(−) and treated with α-MEM(−) (200 μL) containing 10 μM FITC-R8 in the presence or absence of 40 μM peptide at 37 °C under 5 % CO_2 for 5 min. Note that to analyze the interaction of the peptides with the membrane more accurately and to avoid the potential effect of serum proteins and other materials on peptide-membrane interaction, serum-free medium [α-MEM(−)] was consistently employed in this study. After the incubation, cells were twice washed with phosphate-buffered saline (PBS) containing heparin sodium (0.5 mg/mL), and α-MEM(+) (1mL) was added prior to observation. The intracellular distribution of FITC-R8 was analyzed using an Olympus FV 1000 CLSM equipped with a 40× objective.

For the experiments shown in Figure S3, HeLa cells were plated as above. Cells were twice washed with α-MEM(−) and incubated with α-MEM(−) (150 μL). Next, cells were treated by adding 50 μL of an α-MEM(−) solution supplemented with 40 μM FITC-R8 and 160 μM peptide (4x solution). Procedure (1:3 dilution) should yield 10 μM and 40 μM at the final concentration, respectively, and dishes with cells were incubated at 37 °C under 5 % CO_2 for 5 min. After the incubation, cells were twice washed with PBS containing heparin sodium (0.5 mg/mL), and α-MEM(+) (1mL) was added prior to observation. The intracellular distribution of FITC-R8 was analyzed using an Olympus FV1000 CLSM equipped with a 40× objective.

Table 1. Sequences of EpN18 analogs and their characterization.

Peptide	Sequence	$[\theta]_{222}$ [a]	$[L]_{1/2}$ [b]	R_t [c]	ΔT_H [d]
EpN18	XSTSSLRRQXKNIVHNYS–amide	-2.6×10^4	N.D.	25.7	9.3
EpN18-L6W	XSTSSWRRQXKNIVHNYS–amide	-1.7×10^4	169.4	25.3	8.1
EpN18-L	LSTSSWRRQLKNLLHNLS–amide	-3.0×10^4	29.7	32.0	10.7
EpN18-V	VSTSSWRRQVKNVVHNVS–amide	-1.1×10^4	N.D.[e]	21.1	3.2
EpN18-Q	XQQQQWRRQXKQIVHQYQ–amide	N.D.[e]	N.D.[e]	24.3	4.0
EpN18-N	XNNNNWRRNXKNIVHNYN–amide	-6.7×10^3	2029.7	22.4	2.7
EpN18-K	XSTSSWKKQXKNIVHNYS–amide	-1.7×10^4	287.5	24.8	5.0
EpN18-R	XSTSSWRRQXRNIVHNYS–amide	-2.0×10^4	132.5	26.1	2.5

[a]molar ellipticity at 222 nm (deg cm^2 $dmol^{-1}$), [b]peptide concentration to yield 50% saturation (μM), [c]retention times in HPLC (min), [d]difference in L_α-to-H_{II} phase transition temperature (T_H) (°C), [e]not determined.

Conflicts of interest

There are no conflicts to declare.

Acknowledgements

This work was supported by JSPS KAKENHI (Grant Numbers, 18H04547 and 20H04707). This work was also supported by the International Collaborative Research Program of the Institute for Chemical Research, Kyoto University (Grant Numbers, 2020-68, 2021-81, and 2022-77).

Keywords: curvature • epsin-1 • lipid packing • membranes • peptides

References

[1] H. T. McMahon, J. L. Gallop, *Nature* **2005**, *438*, 590-596.

[2] a) H. T. McMahon, E. Boucrot, *J. Cell Sci.* **2015**, *128*, 1065-1070; b) I. K. Jarsch, F. Daste, J. L. Gallop, *J. Cell Biol.* **2016**, *214*, 375-387; c) M. Kitamata, T. Inaba, S. Suetsugu, *Biochem. Soc. Trans.* **2020**, *48*, 837-851.

[3] a) M. M. Kozlov, J. W. Taraska, *Nat. Rev. Mol. Cell Biol.* **2023**, *24*, 63-78; b) C. Steinem, M. Meinecke, *Soft Matter* **2021**, *17*, 233-240.

[4] T. Itoh, P. De Camilli, *Biochim Biophys Acta* **2006**, *1761*, 897-912.

[5] a) A. Lamazière, C. Wolf, O. Lambert, G. Chassaing, G. Trugnan, J. Ayala-Sanmartin, *PLoS One* **2008**, *3*, e1938; b) J. A. Jackman, V. V. Costa, S. Park, A. Real, J. H. Park, P. L. Cardozo, A. R. Ferhan, I. G. Olmo, T. P. Moreira, J. L. Bambirra, V. F. Queiroz, C. M. Queiroz-Junior, G. Foureaux, D. G. Souza, F. M. Ribeiro, B. K. Yoon, E. Wynendaele, B. De Spiegeleer, M. M. Teixeira, N. J. Cho, *Nat. Mater.* **2018**, *17*, 971-977; c) T. Murayama, T. Masuda, S. Afonin, K. Kawano, T. Takatani-Nakase, H. Ida, Y. Takahashi, T. Fukuma, A. S. Ulrich, S. Futaki, *Angew. Chem. Int. Ed. Engl.* **2017**, *56*, 7644-7647.

[6] a) T. Masuda, H. Hirose, K. Baba, A. Walrant, S. Sagan, N. Inagaki, T. Fujimoto, S. Futaki, *Bioconjug. Chem.* **2020**, *31*, 1611-1615; b) S. Afonin, A. Frey, S. Bayerl, D. Fischer, P. Wadhwani, S. Weinkauf, A. S. Ulrich, *Chemphyschem* **2006**, *7*, 2134-2142.

[7] a) K. Matsuzaki, K. Sugishita, N. Ishibe, M. Ueha, S. Nakata, K. Miyajima, R. M. Epand, *Biochemistry* **1998**, *37*, 11856-11863; b) S. Guha, J. Ghimire, E. Wu, W. C. Wimley, *Chem. Rev.* **2019**, *119*, 6040-6085.

[8] G. Drin, B. Antonny, *FEBS Lett.* **2010**, *584*, 1840-1847.

[9] H. Chen, S. Fre, V. I. Slepnev, M. R. Capua, K. Takei, M. H. Butler, P. P. Di Fiore, P. De Camilli, *Nature* **1998**, *394*, 793-797.

[10] S. Pujals, H. Miyamae, S. Afonin, T. Murayama, H. Hirose, I. Nakase, K. Taniuchi, M. Umeda, K. Sakamoto, A. S. Ulrich, S. Futaki, *ACS Chem. Biol.* **2013**, *8*, 1894-1899.

[11] a) F. Campelo, H. T. McMahon, M. M. Kozlov, *Biophys. J.* **2008**, *95*, 2325-2339; b) M. G. Ford, I. G. Mills, B. J. Peter, Y. Vallis, G. J. Praefcke, P. R. Evans, H. T. McMahon, *Nature* **2002**, *419*, 361-366; c) T. Itoh, S. Koshiba, T. Kigawa, A. Kikuchi, S. Yokoyama, T. Takenawa, *Science* **2001**, *291*, 1047-1051.

[12] W. Y. Hsu, T. Masuda, S. Afonin, T. Sakai, J. V. V. Arafiles, K. Kawano, H. Hirose, M. Imanishi, A. S. Ulrich, S. Futaki, *Bioorg. Med. Chem. Lett.* **2020**, *30*, 127190.

[13] K. Kuroki, T. Sakai, T. Masuda, K. Kawano, S. Futaki, *Bioorg. Med. Chem. Lett.* **2021**, *43*, 128103.

[14] C. Has, S. L. Das, *Biochim. Biophys. Acta Gen. Subj.* **2021**, *1865*, 129971.

[15] N. Wang, L. D. Clark, Y. Gao, M. M. Kozlov, T. Shemesh, T. A. Rapoport, *Nat. Commun.* **2021**, *12*, 568.

[16] a) L. Vamparys, R. Gautier, S. Vanni, W. F. Bennett, D. P. Tieleman, B. Antonny, C. Etchebest, P. F. Fuchs, *Biophys. J.* **2013**, *104*, 585-593; b) B. Nepal, J. Leveritt, 3rd, T. Lazaridis, *Biophys. J.* **2018**, *114*, 2128-2141; c) K. D. Wildermuth, V. Monje-Galvan, L. M. Warburton, J. B. Klauda, *J. Chem. Theory Comput.* **2019**, *15*, 1418-1429; d) N. S. Hatzakis, V. K. Bhatia, J. Larsen, K. L. Madsen, P. Y. Bolinger, A. H. Kunding, J. Castillo, U. Gether, P. Hedegård, D. Stamou, *Nat. Chem. Biol.* **2009**, *5*, 835-841; e) A. H. Larsen, *Int. J. Mol. Sci.* **2022**, *23*; f) R. V. M. Freire, Y. Pillco-Valencia, G. C. A. da Hora, M. Ramstedt, L. Sandblad, T. A. Soares, S. Salentinig, *J. Colloid Interface Sci.* **2021**, *596*, 352-363; g) M. Siggel, R. M. Bhaskara, M. K. Moesser, D. I. I, G. Hummer, *J. Phys. Chem. Lett.* **2021**, *12*, 1926-1931; h) S. Vanni, L. Vamparys, R. Gautier, G. Drin, C. Etchebest, P. F. Fuchs, B. Antonny, *Biophys J* **2013**, *104*, 575-584; iN. van Hilten, K. S. Stroh, H. J. Risselada, *J. Chem. Theory Comput.* **2022**, *18*, 4503-4514.

[17] M. Giménez-Andrés, A. Čopič, B. Antonny, *Biomolecules* **2018**, *8*.

[18] K. Matsuzaki, O. Murase, H. Tokuda, S. Funakoshi, N. Fujii, K. Miyajima, *Biochemistry* **1994**, *33*, 3342-3349.

[19] G. Drin, J. F. Casella, R. Gautier, T. Boehmer, T. U. Schwartz, B. Antonny, *Nat. Struct. Mol. Biol.* **2007**, *14*, 138-146.

[20] E. T. Kaiser, F. J. Kézdy, *Science* **1984**, *223*, 249-255.

[21] a) P. Y. Chou, G. D. Fasman, *Biochemistry* **1974**, *13*, 211-222; b) T. E. Creighton, *Proteins: structures and molecular properties (Second edition)*, W. H. Freeman, **1992**.

[22] a) W. F. Degrado, *Adv. Protein. Chem.* **1988**, *39*, 51-124; b) I. V. Korendovych, W. F. DeGrado, *Q. Rev. Biophys.* **2020**, *53*, e3.

[23] Y. I. González, H. Nakanishi, M. Stjerndahl, E. W. Kaler, *J. Phys. Chem. B* **2005**, *109*, 11675-11682.

[24] a) C. D. Chang, J. Meienhofer, *Int. J. Pept. Protein Res.* **1978**, *11*, 246-249; b) S. Futaki, M. Fukuda, M. Omote, K. Yamauchi, T. Yagami, M. Niwa, Y. Sugiura, *J. Am. Chem. Soc.* **2001**, *123*, 12127-12134.

[25] R. Gautier, D. Douguet, B. Antonny, G. Drin, *Bioinformatics* **2008**, *24*, 2101-2102.

[26] R. W. Woody, *Methods Enzymol.* **1995**, *246*, 34-71.

[27] J. W. Nelson, N. R. Kallenbach, *Proteins* **1986**, *1*, 211-217.

[28] J. Allen, J. P. Pellois, *Sci. Rep.* **2022**, *12*, 15981.
[29] a) R. M. Epand, K. D'Souza, B. Berno, M. Schlame, *Biochim. Biophys. Acta* **2015**, *1848*, 220-228; b) J. Jouhet, *Front. Plant. Sci.* **2013**, *4*, 494.
[30] D. M. Owen, C. Rentero, A. Magenau, A. Abu-Siniyeh, K. Gaus, *Nat. Protoc.* **2011**, *7*, 24-35.
[31] R. W. Glaser, A. S. Ulrich, *J. Magn. Reson.* **2003**, *164*, 104-114.

Entry for the Table of Contents

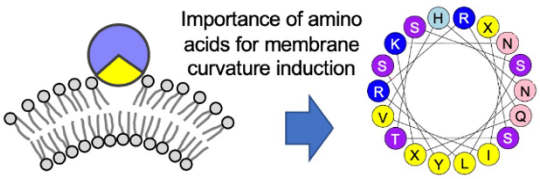

The induction of local changes in membrane structure often plays a pivotal role for cellular life. Epsin-1 is a representative protein to induce positive membrane curvature and its N-terminal segment (EpN18) plays a key role. This study aimed to elucidate the essential structural features of EpN18 for a better understanding of general curvature-modulating mechanisms and to design effective tools for rationally controlling membrane structure.